Needle Path Planning for Digital Breast Tomosynthesis Biopsy

Laurence Vancamberg, Anis Sahbani, Serge Muller and Guillaume Morel

***Abstract*— This paper presents a new needle path planning method for digital breast tomosynthesis biopsy. Needle insertion planning into deformable tissue for breast biopsy procedure is a challenging task because of the infinite possibilities of insertion points. In addition, the lesion moves from its original position when the radiologist introduces the biopsy needle. The proposed approach couples Rapidly-exploring Random Trees with Finite Element Simulation in order to find an optimal path taking breast deformations into account. Simulation results show that this method reduces the error (*i.e.* the distance between the needle tip and the lesion) by 80 %.**

I. INTRODUCTION

Breast cancer is one of the most common cancers among women. Today, specialists estimate that one woman over 8 will be touched by a breast cancer [1]. After the screening step, the radiologist may collect samples of suspect tissues through a biopsy to evaluate if the lesion is benign or malignant. This procedure can be guided by ultrasound or by X-ray stereotaxy, depending on the type of lesions, respectively masses or calcifications. In the US, 8% to 10% of women who have a mammogram will need a biopsy [2]. In addition, mammography has been advancing considerably along with the development of digital breast tomosynthesis (DBT). The introduction of this modality can offer new possibilities for screening and diagnosis but also for needle biopsy procedures. The 3D reconstruction gives access to spatial coordinates of any point in the breast instead of having only the 3D coordinates of the target point with the classic stereotaxy procedure.

Stereotactic biopsy system faces some drawbacks like non-optimized needle path. The only criterion used to choose the device path is the lesion position into a breast quadrant. This non-optimized planning can have undesirable consequences, like bleedings when the needle hits a vessel. Furthermore, today stereotactic guidance devices can not be moved during the needle insertion : the orientation of the needle along its axis can not be controlled and only a translation along the needle axis is allowed, reducing the range of possible needle paths. Figure 1 illustrates the constraints of a stereotactic guidance device.
In addition, even if the breast is compressed, the lesion moves from its original position when the radiologist introduces the biopsy needle [3]. He doesn't know exactly where the target is when he performs the intervention and the samples he takes can be non representative. The radiologist has to redo the insertion causing patient discomfort.

L. Vancamberg is with GE Healthcare, Buc, France and with ISIR-CNRS, Pierre & Marie Curie University, Paris 6, UMR 7222, F-75005, France. laurence.vancamberg@ge.com

S. Muller is with GE Healthcare, Buc, France. serge.muller@ge.com

A. Sahbani and G. Morel are with ISIR-CNRS, Pierre & Marie Curie University, Paris 6, UMR 7222, F-75005, France. anis.sahbani@upmc.fr, morel@robot.jussieu.fr

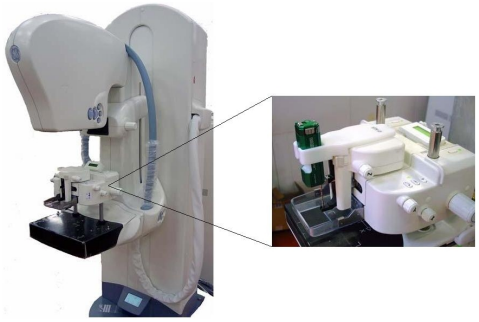

Fig. 1. GE Healthcare Senographe DS Interventional and its stereotactic positioner (vertical approach). Only a translation along the needle axis is permitted.

Aware of this limitations, we want to find an optimal insertion point and an optimal needle path taking into account breast deformations and the kinematic and kinetic constraints of the needle. This task is challenging because of the infinity of possible initial needle configurations q_{init} on the breast surface and because of the mutual influence between the initial needle configuration q_{init} and the goal needle configuration q_{goal}. Actually, we want to find an optimal insertion point q^*_{init} knowing the target point coordinates *i.e.* to define a function f such as : $q^*_{init} = f(q_{goal})$, but because of breast deformations during needle insertion, the final needle configuration depends on the needle path: $q_{goal} = g(q_{init})$.

As in our application the rotation of the needle along its axis is fixed during the insertion, we focus on non-steerable symmetric stiff and bevel-tip flexible needles. We did not consider steerable needles because the diameter of breast biopsy needles is up to 9 Gauge, reducing considerably the bending effect. This forces us to consider the bending of the needle as an undesirable effect rather than as an asset to reach the target.

The present paper is organized as follows. Section II describes the related work. Then in section III, the proposed approach to find an optimal needle path is detailed. In section IV, tests that have been made to validate our method, are presented. Finally, Section V explains the future works.

II. Related Works

Lots of research have been made related to needle insertion and lesion displacements problems. Three different categories of approaches have been investigated to address these problems: motion planning methods, soft tissues deformations simulation methods and methods combining the two previous ones.

Needles can be considered as kinematic systems with nonholonomic constraints [4]. Motion planning methods are often used to determine 2D or 3D paths (a sequence of insertions and direction changes) for steerable needles, such as the needle tip reaches the specified target while avoiding obstacles [5] [10].
Alterovitz *et al.* [5] [6] find optimal paths considering uncertainty and discrete configuration states of the steerable needle. However these methods are only applicable in a planar situation.
The first 3D path planning method, using a diffusion-based approach, was introduced by Park *et al.* [7] but only considered obstacle free 3D environments.
Since then, other 3D approaches avoiding obstacles based on various algorithms have been proposed : Duindam *et al.* considered the problem as a dynamical optimization problem with a discretization of the control space [8]. They also proposed a solution based on inverse kinematics [9]. In [10], Xu *et al.* developed a solution based on Rapidly-exploring Random Trees (RRTs) that builds a global roadmap starting from the goal configuration.
Nevertheless all these approaches are not directly applicable to our problem. First of all, most of them assume a defined initial configuration. In addition, the needle has more degrees of freedom (rotation along its axis). And more important, these approaches do not take into account soft tissue deformations.

Meanwhile a lot of progress has been made in the field of needle insertion simulation. Deformations that occur during needle insertion are often analyzed with finite element (FE) methods. DiMaio and Salcudean proposed a quasi-static version of the FE methods in a planar environment [11]. Alterovitz simulated dynamic 2D deformations of soft materials for rigid needle [12] and bevel-tip needle [13] insertion. In 2004, a first 3D interactive rigid needle insertion simulator *Artisjokke* was developed by Nienhuys and van der Stappen [14] which can compute linear and nonlinear material deformation. More recently a simulator for both symmetric-tip stiff needle and bevel-tip flexible needle insertion was presented by Chentanez *et al.* [15]. Both simulators are based on a stick-slip model of the friction between the tissue and the needle shaft. However these simulators are just used to visualize the soft tissue deformations, they are not coupled with the notion of optimized path.

The last category of approaches groups methods that associate the two concepts described above. The first method coupling motion planning with deformations analysis for rigid needle insertion was proposed by Alterovitz *et al.* [16] in 2003. It consists in testing all 2D trajectories in a feasible range of insertion heights and depths and select the one that minimizes the seed placement error (the Euclidean distance between the final position of the seed and the final position of the target) using a FE analysis. An improvement of the method was proposed for bevel-tip needle insertion using numerical optimization to plan the best path [13]. Di Maio and Salcudean also proposed a method coupling FE analysis and needle motion planning based on potential fields [17]. They translate and orient the base of the needle to avoid obstacles and reach a target point. More recently, Hauser *et al.* implemented a method to reach a 3D target in deformable tissue implementing a feedback control and using helical path [18].
The first two methods are limited to 2D problems. In the other methods, the base of the needle moves to reach the target. As explained above, in our application, we can not rotate the needle or translate the needle except along its axis during the insertion. Consequently all of these methods are not good candidates to solve our problem.

Dehghan *et al.* in [19] proposed an optimization method, based on iterative finite element simulations, that finds an optimal needle path for brachytherapy. In this work, similar constraints as tomosynthesis biopsy are considered. At each iteration, the simulated path minimizes the distance between the rigid needle and displaced targets. Nevertheless, in this paper, the multiple targets define a unique insertion point, whereas in our case, with one target, there is an infinity of possible insertion points. In addition, their numerical optimization doesn't guarantee the respect of the convergence criteria, even if in practice, simulation results shows that it converges in a few iterations.

In this paper, we present a novel approach that couples Rapidly-Exploring Random Tree (RRT) planning methods [20] with finite element simulation to find an optimal path for digital breast tomosynthesis biopsy.

III. Proposed Approach

Our goal is to find an optimal needle insertion point and an optimal needle path constrained by the application specificities: the needle can only be translated along its axis and its orientation is fixed during the insertion, there is no image feedback and we want to have a planning method taking breast deformations into account.

The configuration space that we will consider in the following section is the basis associated with the needle at the needle tip:

$$q = (X, Y, Z, \phi, \theta, \psi)$$

where (X, Y, Z) is the position of the needle tip and (ϕ, θ, ψ) are the Euler angles.

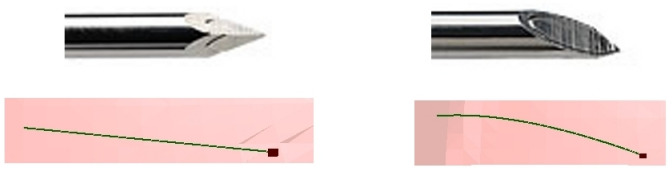

Fig. 2. Trajectories generated by non-steerable needles. Left: a symmetric rigid needle follows a straight line. Right: a bevel-tip flexible needle follows an arc of circle.

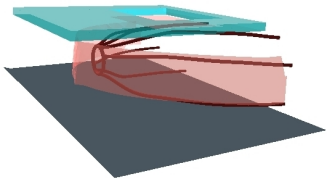

Fig. 3. Graphic interface of Simplan: in blue the compression paddle, in gray the detector, in red the vessels and in pink BS' a part of the breast surface where the needle can be inserted.

In our particular application, two types of needle trajectories are generated. A symmetric-tip needle exerts forces on the tissue equally in all directions so it follows a straight line when it is inserted into homogeneous tissue. A bevel-tip needle exerts forces asymmetrically and bends in the direction of the bevel. It follows an arc of circle whose curvature depends on the needle itself and tissue characteristics [4]. Figure 2 describes the different types of needle trajectories.

The proposed approach consists in three steps:

- Without taking breast deformations into account, a low-cost needle path is computed.
- Then a family of optimal candidate paths is generated from this low-cost path.
- Finally the needle insertions along these paths are simulated in order to select the optimal one.

Each step will be detailed in the following subsections.

A. Insertion Point and Needle Path Research with Relaxed Constraints

The first step of our approach is to find an optimal needle path P' with relaxed constraints: we are searching a path from a region of the breast surface to the target considering the breast as undeformable.

From the DBT reconstructed volume, a triangular mesh of the patient breast surface BS can be generated. In our application, the radiologist selects in a slice of the DBT reconstructed volume the lesion (s)he wants to biopsy. The 3D position of the target $L = (X_t, Y_t, Z_t)$ is calculated directly from the number of the slice n and the i and j coordinates of the selected pixel.
Knowing the geometry of the DBT system and the biopsy positioner, we define a subset of BS, BS' that the needle can reach. Figure 3 illustrates the patient-specific graphic environment, build from the DBT acquisition and the knowledge of the DBT system.

We are also searching a path going from an initial configuration:

$$q_{init} = (X_i, Y_i, Z_i, \phi_i, \theta_i, \psi_i)$$

where $(X_i, Y_i, Z_i) \in BS'$, to a final configuration:

$$q_{goal} = (X_t, Y_t, Z_t, \phi_t, \theta_t, \psi_t).$$

Usual planning methods enable to find a path between an initial configuration and a goal configuration. But in our case we have an infinity of possible q_{init}: any point of the breast surface with orientations $(\phi_i, \theta_i, \psi_i)$ that can be accessed by the needle tip are initial configuration candidates. In fact, the goal configuration is not completely determined : only the position of the lesion (X_t, Y_t, Z_t) is known, but the orientation of the needle reaching the target, $(\phi_t, \theta_t, \psi_t)$, has to be determined.

The use of Rapidly Exploring Random Trees (RRT) methods [20] with backchaining is particularly well-suited for steerable needles path planning [10]. The backchaining planning finds a path starting from the goal configuration q_{goal} to the initial configuration q_{init}. The tree grows backward from the target to explore the configuration space, by applying negative control inputs.
We have adapted this algorithm to improve its efficiency for symmetric stiff needles and bevel-tip flexible needles. Two modifications are presented below.

To ensure the patient comfort, we have chosen to modelize vessels like obstacles in the modified RRT algorithm. The needle path is constrained to be at a security distance s from the vessels:

$$s = D * (1 + \lambda) \qquad \lambda \in [0, 1].$$

where D is the needle diameter and λ a security parameter. We made synthetic vessels schematically representing the surface vessel network [21].

In digital breast tomosynthesis biopsy, the orientation of the needle is fixed during the intervention. We consider that the insertion speed is constant. Therefore, the number of control inputs u in the negative control space $-U$ that we can apply for a given configuration to generate is reduced to only one. Given a desired input u, *i.e.* the needle insertion speed, a path going from q_{goal} to BS' can be generated using the following algorithm.

Algorithm 1: the root R of the tree T is initialized as q_{goal}. Instead of stopping T growing when it reaches a region like in [10], T stops growing when it collides with the breast surface BS'. A randomly sampled collision free state q_{rand} is generated and q_{near} the nearest neighbor in T is selected. A new state is then generated but as the orientation of

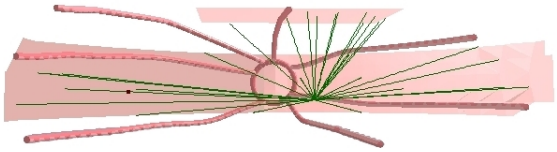

Fig. 4. Step A: Generation of a set S of paths with the exploring version of our algorithm.

q_{goal} is not fixed NEW_STATE() becomes: if $q_{near} = R$, the input u is applied to all possible goal configurations. A set Q_{new} of possible new states is obtained and the nearest neighbor of q_{rand} in Q_{new} is found as q_{new} which is totally determined. Else ($q_{near} \neq R$), we apply the input u to q_{near} to have q_{new}. q_{new} is computed using a control input function $G_{q_{near}}(u)$, which depends on the needle type: for rigid needles, $G_{q_{near}}(u)$=$-u$, for flexible needles, $G_{q_{near}}(u)$ depends on the needle curvature. Then q_{new} is added to T using ADD_NODE(). To ensure the fast convergence of the algorithm, ADD_NODE(), in addition to add the vertex and the edge, marks q_{near} as not selectable except if it concerns R. If a configuration is not selectable, it will not be taken into account for the nearest reachable neighbor research. Thus, there is no duplicate configurations in the tree T.

However, we have noticed that this algorithm was not explorative : the number of branches of the tree was quite small. An improvement of this method is exposed below.

Algorithm 2: in order to optimize the previous algorithm and to take into account the mentioned limitation, the NEAREST_REACHABLE_NEIGHBOR() function is modified. It forces now the algorithm to choose the tree root R as the nearest neighbour with a frequency f. The consequence is a creation of new branches.
Table I details the modified RRT algorithm.

Our algorithm stops when it gives us a desired number of possible paths S going from the breast surface to the lesion avoiding the vessels. Figure 4 shows 30 paths found with the modified RRT algorithm. The breast is seen from the chest wall (right of Fig. 3).

Then, we have defined a cost function C. For each path $P \in S$, a cost c is computed. C can depend on many parameters based on the preference of radiologists: length of P, distance to the vessels, reduction of image artefacts, proximity of the chest wall, ... An example of cost function is:

$$C(P) = -\alpha * min_{n_i \in P}(d(n_i, Obst)) + (1-\alpha) * l(P)$$

where n_i are the nodes of the path P, d is a metric measuring the distance between the nodes and the obstacles, l is the length of the path and α a weighting factor.
The lowest cost path P' is selected :

$$P' = min_{P \in S}(c)$$

TABLE I

EXPLORING VERSION OF THE MODIFIED RRT ALGORITHM

```
BUILD_RRT(q_goal, BS')
1. T = T_init(q_goal)
2. while T ∩ BS' = ∅
3.         q_rand ← RANDOM_STATE()
4.         T ← EXTEND(T,q_rand)
5. END

EXTEND(T,q_rand)
1. q_near ←NEAREST_REACHABLE_NEIGHBOR(T,q_rand)
2. q_new ← NEW_STATE(q_near,q_rand,U)
3. T.ADD_NODE(q_near,q_new,U)
4. return T

NEAREST_REACHABLE_NEIGHBOR(T,q_rand)
1. num ← RANDOM([0,1])
2. if (num > f)
3.         for all q_i ∈ T
4.             if q_rand is reachable from q_i and dist(q_i,q_rand) < dist
5.                 q_near = q_i
6. else
7.         q_near = R
8. RETURN q_near

NEW_STATE(q_near,q_rand,U)
1. if q_near = R
2.         for all q_goal orientations
3.             q_new(o) = q_goal + G_q_goal(u)δt
4.         Q_new = ∪_o q_new(o)
5.         q_new ← NEAREST_NEIGHBOR(Q_new, q_rand)
6. else
7.         q_new = q_near + G_q_near(u)δt
8. RETURN q_new
```

A first low-cost path P' is then found with relaxed constraints.

However, if we simulate the needle insertion for P' taking into account the deformations of the breast, the lesion will move. The final position of the needle tip $p'_{goal} = (X'_f, Y'_f, Z'_f) = (X_t, Y_t, Z_t)$ and the final position of the lesion $L' = (X'_t, Y'_t, Z'_t)$ will be different.
To solve this issue, we propose to generate from P' a particular family $F_{p'}$ of paths and simulate the needle insertion along them.

B. Multiple candidate paths generation

The goal now is to find an optimal path P^* taking breast deformations into account. We seek to minimize the error e defined as the Euclidean distance between the final position of the needle tip $p_{goal} = (X_f, Y_f, Z_f)$ and the final position of the target $L_f = (X_{t_f}, Y_{t_f}, Z_{t_f})$.

We first simulate the insertion of the needle following the low-cost path P'. The used technique for this simulation is presented in the next section. The final position of the target $L' = (X'_t, Y'_t, Z'_t)$ is recorded. We define a zone $Z_{L'}$ around L'. Then multiple paths are generated going from configurations around q'_{init} to configurations where $p_{goal} \in Z_{L'}$.The idea is that for a path P similar to P' the lesion will arrive in this zone $Z_{L'}$ because the lesion and the breast tissues will

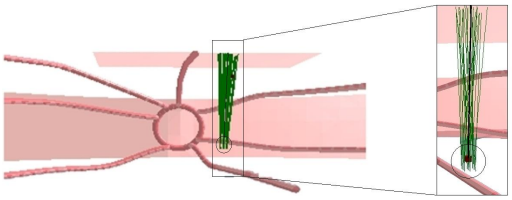

Fig. 5. Step B: Generation of candidate paths family starting from $Z_{L'}$.

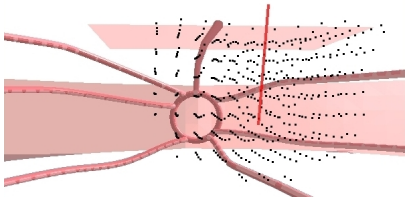

Fig. 6. Step C: Needle insertion simulation.

be subjected to similar forces. We also want to find many possible paths around P' and test them.
To obtain these multiple candidates, we use once again a version of a backchaining RRT algorithm to generate multiple trees growing from $Z_{L'}$. We discretize the zone to get a set of new goal configurations. Then we find for every $q_{goal} \in Z_{L'}$ a path going from q_{goal} to the breast surface BS'. We control that the difference of orientations between every $q_{goal} \in Z_{L'} : o_{goal} = (\phi_t, \theta_t, \psi_t)$ and $q'_{goal} : o'_{goal} = (\phi'_t, \theta'_t, \psi'_t)$ is small enough to have a path similar to P'. To achieve that, the algorithm rejects any root configuration where $o_{goal} - o'_{goal} > \varepsilon$. For steerable needles, constraining only the goal configuration orientation is not sufficient. The difference of orientation between every node of P and its corresponding node in P' has to be small enough.
As these paths are similar to P', the value of the cost function should not be so different from the optimal one found without breast deformations. Nevertheless, a candidate path P may happen to be running very close to an obstacle (*e.g.*, a vessel) and will entail an increased cost. To insure that all candidate paths have a reasonable cost, we can reject P if c is too high.

We finally get a family $F_{p'}$ of paths arriving in the zone of interest with an acceptable cost. Figure 5 illustrates a family of path generated from a lower-cost path P' represented in black. We will now simulate the needle insertion for every path of this family.

C. Needle insertions simulation

We now want to link the motion planning and the simulation of tissue deformation. We have chosen to use Finite Element (FE) methods to simulate breast deformations and needle insertion. FE methods are often used for continuum mechanics and to analyze deformations of anatomical parts [22].

The geometry input of our software is a patient specific 3D model of the breast. The DBT reconstruction allows the creation of a patient specific tetrahedric mesh that we generate using VTK.
We constrain the nodes linked to the chest wall and to the detector to be motionless. We also associate Young's Modulus to the nodes of the FE mesh in order to describe the material biomechanical properties. The value of this coefficient can be found in [23]. In our current implementation, we consider breast tissue as linear, homogeneous and isotropic soft tissue. The hypothesis of homogeneous breast tissue can appear as totally inexact but research on breast tissue properties have shown that when the breast is compressed enough the fat Young's Modulus increases becoming equal to the Young's Modulus of glandular tissue [24]. Azar argues that the stiffness value increases because of Cooper's ligaments that compartmentalize the fatty tissue in the breast and prevent it from being squeezed out of its location.

To compute soft tissue deformations, we modified Artisjokke simulator [14] to create a patient specific application. Forces resulting from needle insertion deform the mesh and we can automatically simulate the insertion of the needle for every path $P \in F_{p'}$. Figure 6 represents mesh deformations during a needle insertion simulation. The software also measures automatically the distance between the final position of the needle tip $p_{goal} = (X_f, Y_f, Z_f)$ and the final position of the lesion $L_f = (X_{t_f}, Y_{t_f}, Z_{t_f})$ obtained for this path with the deformations of the mesh:

$$e = (X_f, Y_f, Z_f) - (X_{t_f}, Y_{t_f}, Z_{t_f}).$$

The optimal path is the one that minimizes the error:

$$P^* = min_{P \in F_{p'}}(e).$$

We proposed a complete approach providing a solution to our problem. A low-cost path with relaxed constraints P' is computed. Then multiple paths $F_{p'}$ are generated and tested using the simulator. Finally, the best path P^* that minimizes the final distance between the needle tip and the target is selected. In order to evaluate the efficiency of our approach, a set of experiments detailed in next section are conducted.

IV. Experimental Results

We implemented our new algorithm adapting and coupling the classical RRT algorithm using the Motion Strategy Library (MSL) and Artisjokke [14].
Even if our planning approach is still valid for steerable needles, experimental simulations are conducted for non-steerable needles (symmetric stiff and bevel-tip flexible needles) in order to evaluate the presented method.

To evaluate the pertinence of our method, we performed a DBT exam on a breast stereotactic phantom (CIRS). We located 13 lesions inside this phantom and applied our algorithm for all of them. We obtained a 26935 tetrahedra mesh and we added synthetized vessels.

TABLE II

ALGORITHM EVALUATION

Lesion number	1	2	3	4	5	6	7
e' (mm)	1.29	0.53	0.64	1.08	1.80	2.18	3.18
e* (mm)	0.24	0.11	0.18	0.38	0.83	0.64	0.52
Lesion number	8	9	10	11	12	13	
e' (mm)	2.41	1.08	1.45	2.35	1.73	1.38	
e* (mm)	0.06	0.24	0.15	0.10	0.12	0.37	

The performance of our method was evaluated by comparing the error, e' obtained for the optimal path without breast deformations P' and the error, e^* generated by P^* found with our planning method. The comparison was made for the 13 different positions of the target. The results, presented in Table II, show that our method reduces the error meanly by 80 % with a standard deviation of 13%.

The mean planning time is 15.3 seconds to generate a set S of 30 paths (step A) and 5.0 seconds to generate a family $F_{p'}$ of 27 paths (step B). In fact the planning time is negligible in comparison to the simulation time. The time needed to simulate a needle insertion is between 30 seconds and 80 seconds, which means that the entire procedure takes approximately 20 minutes on an Intel Core2 Duo 2.40GHz 5GB Ram PC.

V. CONCLUSION AND FUTURE WORKS

In this paper, we have proposed a novel method combining RRTs algorithm with FE analysis to find an optimal insertion point and needle path in a 3D environment. The tissue deformations is taken into account for the path choice. This method uses DBT volumetric capabilities to create a patient specific application. We have shown that with our algorithm the error due to breast tissue displacements is reduced meanly by 80 %.

In future work, we will build a specific method for non-steerable needles, based on breast surface sampling, instead of sampling randomly from the configuration space. Part of our perspective work is to evaluate the simulation accuracy. We plan to compare the simulation results with the deformations obtained on an anthropomorphic biopsy phantom. Up to now, we only used 3D synthetic vessels but work is going to automatically segment the vessels from the DBT slices in order to get realistic and patient-specific obstacles.

VI. ACKNOWLEDGMENTS

This work has been partially funded by ANRT under CIFRE grant n^o1035/2008. We thank the reviewers for their valuable comments.

REFERENCES

[1] American Cancer Society, "Breast Cancer Facts & Figures 2007-2008".

[2] American Cancer Society, "American Cancer Society: Breast Cancer", *http://documents.cancer.org/104.00/104.00.pdf*, 2009.

[3] E. Deurloo, K. Gilhuijs, L. Kool and S. Müller, "Displacement of breast tissue and needle deviation during stereotactic procedures", *Investigative Radiology*,vol. 36, 2001, pp 347-353.

[4] R.J. Webster III, N.J. Cowan, G. Chirikjian and A.M. Okamura, "Nonholonomic Modeling of Needle Steering", *9th International Symposium on Experimental Robotics*, Singapore, 2004.

[5] R. Alterovitz,A. Lim, K. Goldberg, G.S. Chirikjian and A.M. Okamura, "Steering Flexible Needles Under Markov Motion Uncertainty", *IEEE International Conference on Intelligent Robots and Systems (IROS)*, 2005, pp. 120-125.

[6] R. Alterovitz,M. Branicky and K. Goldberg, "Constant-Curvature Motion Planning Under Uncertainty with Applications in Image-Guided Medical Needle Steering", *Workshop on the Algorithmic Foundations of Robotics*, 2006.

[7] W. Park, J.S. Kim, Y. Zhou, N.J. Cowan, A.M. Okamura and G.S. Chirikjian, "Diffusion-Based Motion Planning for a Nonholonomic Flexible Needle Model",*IEEE International Conference on Robotics and Automation (ICRA)*, 2005 .

[8] V. Duindam, R. Alterovitz, S. Sastry and K. Goldberg, "Screw-Based Motion Planning for Bevel-Tip Flexible Needles in 3D Environments with Obstacles", *IEEE International Conference on Robotics and Automation (ICRA)*, 2008.

[9] V. Duindam, Jijie Xu, R. Alterovitz, S. Sastry and K. Goldberg, "3D Motion Planning Algorithms for Steerable Needles Using Inverse Kinematics", *8th Workshop on the Algorithmic Foundations of Robotics*, 2008.

[10] Jijie Xu, V. Duindam, R. Alterovitz and K. Goldberg, "Motion Planning for Steerable Needles in 3D Environments with Obstacles Using Rapidly-Exploring Random Trees and Backchaining", *IEEE Int. Conf. on Automation Science and Engineering (CASE)*, 2008.

[11] S.P. DiMaio and S.E. Salcudean, "Needle Insertion Modeling and Simulation", *IEEE Trans. on Robotics and Automation*, vol. 19, 2003.

[12] R. Alterovitz, K. Goldberg, J. Pouliot, R. Taschereau and I. Hsu, "Needle Insertion and Radioactive Seed Implantation in Human Tissues: Simulation and Sensivity Analysis", *IEEE International Conference on Robotics and Automation (ICRA)*, 2003.

[13] R. Alterovitz, K. Goldberg and A. Okamura, "Planning for Steerable Bevel-tip Needle Insertion Through 2D Soft Tissue with Obstacles", *IEEE International Conference on Robotics and Automation (ICRA)*, 2005, pp. 1652-1657.

[14] H.W. Nienhuys A.F. van der Stappen, "A computational technique for interactive needle insertions in 3D nonlinear material", *IEEE International Conference on Robotics and Automation (ICRA)*, 2004.

[15] N. Chuntanez, R. Alterovitz, D. Ritchie, L. Cho, K.K Hauser, K. Goldberg, J.R. Shewchuk and J.F. O'Brien, "Interactive Simulation of Surgical Needle Insertion and Steering", *SIGGRAPH 2009*, 2009.

[16] R. Alterovitz, K. Goldberg, J. Pouliot, R. Taschereau and I. Hsu, "Sensorless Planning for Medical Needle Insertion Procedures", *IEEE International Conference on Intelligent Robots and Systems (IROS)*, 2003, pp. 3337-3343.

[17] S.P. DiMaio and S.E. Salcudean, "Needle Steering and Motion Planning in Soft Tissues", *IEEE Trans. on Biomedical Engineering*, 2004.

[18] K. Hauser, R. Alterovitz, N. Chentanez, A. Okamura and K. Goldberg, "Feedback Control for Steering Needles Through 3D Deformable Tissue Using Helical Paths", *Robotics: Science and Systems V*, 2009.

[19] E. Dehghan and S.E. Salcudean, "Needle Insertion Parameter Optimization for Brachytherapy", *IEEE Trans. on Robotics*, 2009, vol.25, pp. 303-315.

[20] S.M. LaValle and J. Kuffner, "Rapidly-Exploring Random Trees: Progress and Prospects", *Workshop on the Algorithmic Foundations of Robotics*, 2000.

[21] J.P. Chevrel, *Le Tronc*, Anatomie Clinique, vol. 2, Springer-Verlag, 1994.

[22] S. Cotin, H. Delingette and N. Ayache, "Real-Time Elastic Deformations of Soft Tissues for Surgery Simulation", *IEEE Transactions On Visualization and Computer Graphics*, 1999.

[23] T.A Krouskop, T.M. Wheeler, F. Kallel, B.S. Garra and T. Hall, "Elastic Moduli of Breast and Prostate Tissues Under Compression", *Ultrasonic Imaging*, vol. 20, 1998, pp. 260-278.

[24] F.S. Azar, D.N. Metaxas and M.D. Schnall, "A Finite Element Model of the Breast for Predicting Mechanical Deformations during Biopsy Procedures", *IEEE Workshop on Mathematical Methods in Biomedical Image Analysis*, 2000.